

# Photodegradation of Thermoplastic Elastomeric Rubber–Polyethylene Blends

Anil K Bhowmick,<sup>1</sup> J. Heslop, J. R. White

<sup>1</sup>Rubber Technology Centre, Indian Institute of Technology, Kharagpur-721302, India

<sup>2</sup>Department of Mechanical, Materials & Manufacturing Engineering, University of Newcastle upon Tyne, Newcastle upon Tyne, NE1 7RU, United Kingdom

Received 2 March 2001; accepted 30 October 2001

**ABSTRACT:** The photodegradation of a new family of thermoplastic elastomers, based on blends of natural rubber and polyethylene, was studied with laboratory ultraviolet exposures in the unstrained state and under tensile strain (25 and 50%). Strained exposure caused reduction of the strain to failure in subsequent tensile tests. The blends were more resistant to degradation than the natural rubber homopolymer. The introduction of crosslinks (at a low concentration so that the thermoplastic nature of the blends was retained) changed the resistance to photo-oxidation. Two different crosslinking systems were used. When dicumyl peroxide

was used as the crosslinking agent, the resistance to degradation was reduced, whereas the compound containing a sulfur curing system showed improved resistance to photodegradation. Photo-oxidation rather than ozone degradation was found to be the major cause of breakdown, even with samples held in tension. © 2002 Wiley Periodicals, Inc. *J Appl Polym Sci* 86: 2393–2402, 2002

**Key words:** thermoplastic elastomers; rubber–polyethylene blends; photodegradation

## INTRODUCTION

Thermoplastic elastomers present an attractive combination of properties, including ease of processing (by conventional thermoplastics methods), potential for scrap recycling, and ease of property manipulation through composition change.<sup>1,2</sup> Rubber–plastic blends form a class of thermoplastic elastomers with the potential for many applications in engineering and consumer goods.<sup>2</sup> Initial problems with incompatibility of the rubber and plastic components have been largely overcome,<sup>3–5</sup> but further development is required before they can compete as a low-cost alternative for products such as automotive window seals, currently produced from ethylene–propylene–diene rubber.<sup>6</sup> Many of the potential applications for rubber–plastic blends involve outdoor service, and it is of importance to know their sensitivity to weathering. This is the topic of the study reported on here.

Natural rubber (NR) products can degrade rapidly when exposed outdoors, particularly if loaded in tension. The cause of the degradation is often attributed to ozone attack,<sup>7–10</sup> but recent studies by Adam and colleagues have shown that photo-oxidation is often the dominant mechanism,<sup>11–15</sup> as noted earlier by

Dunn.<sup>16</sup> Studies of ultraviolet (UV) photo-oxidation of thermoplastic polymers have shown that tensile stress accelerates degradation,<sup>17–19</sup> and in a preliminary study of a car tire sidewall rubber, it was shown that tensile stress causes significant changes in the degradation behavior.<sup>20</sup> Some of the methods used in the latter study<sup>20</sup> were applied to a new family of thermoplastic elastomeric NR/low-density polyethylene (LDPE) blends, and the results are reported here.

## EXPERIMENTAL

### Materials and blend preparation

NR was supplied by Rubber Board (Kottayam, India). This had a molecular mass of  $780 \times 10^3$ , an intrinsic viscosity (benzene 30°C  $\text{m}^3/\text{kg}$ ) of 0.44, and a Wallace plasticity of 59.0. The polyethylene (PE), which had a melt flow index of 40 g/10 min, was Indothene 16 MA 400, supplied by IPCL (Baroda, India). Some materials were prepared without any crosslinking system; others were crosslinked with either dicumyl peroxide (DCP) or a vulcanization system based on sulfur. DCP was supplied by Hercules Inc. (Wilmington, DE). The blend compositions are given in Table I. Compounds based on the homopolymers but containing DCP (NR/DCP and PE/DCP) were prepared to compare the effect of DCP on the individual components of the blends. All of these compounds were prepared without stabilizers to counter thermal oxidation or photo-oxidation. The effects of such additives were also examined and reported elsewhere.<sup>21</sup>

Correspondence to: J. R. White.

Contract grant sponsor: UK-India Science & Technology Research Fund.

TABLE I  
Compositions of the Rubber-PE Compounds

Code	NR:LDPE	DCP (phr)
70NR30PE	70:30	0
60NR40PE	60:40	0
70NR30PE/DCP	70:30	1
70NR30PE/S*	70:30	
NR/DCP	100:0	1
LDPE/DCP	0:100	1

70NR30PE/S\* contained 2.5 phr zinc oxide, 1 phr stearic acid, 1 phr sulfur, 0.75 phr MBT, and 0.1 phr TMTD.

The mixing of the blends and the pressing into slabs 2 mm thick was described elsewhere.<sup>22</sup> Strips measuring 100 × 12 mm were cut from the slabs for tensile testing and UV exposure.

### UV exposure arrangements

Samples were exposed to UV irradiation in a constant-temperature room set at 30°C and maintained at 30 ± 1°C. The illumination source consisted of pairs of fluorescent tubes type UVA-340 (Q-Panel Company). The intensity and the spectral distribution of the tubes were checked regularly with a Bentham Instruments spectroradiometer. The tubes were replaced if the illumination level fell below the target value. The measurements made by the spectroradiometer confirmed that the UV output matched the spectrum of solar radiation at the Earth's surface fairly closely,<sup>18</sup> as claimed by the tube manufacturer. The output at higher wavelengths was very much lower than solar radiation levels and did not cause serious heating of the samples. The total intensity used was about 1.8 W/m<sup>2</sup> in a wavelength range of 295–320 nm; that is the total radiation below 320 nm, comparable to levels in a hot, sunny climate.<sup>23,24</sup> The illumination provided by the tubes was checked regularly. The samples were supported on a wood surface and exposed on one side only.

UV exposures were also conducted with samples loaded in uniaxial tensile stress relaxation with simple frames that could accommodate up to 15 separate strips simultaneously. This means that load could not be monitored on individual specimens, but this was not regarded as a serious problem in the context of this rather exploratory study. From the results of creep experiments, however, it is evident that a large fraction of the initial applied stress must have relaxed during the exposure in the blends studied here. Stress-relaxation UV exposures were conducted at strains set at 25 and 50%, respectively. Creep under dead weight loading was found to be quite rapid except at low stresses (well below 1 MPa). Samples partially crosslinked by the presence of DCP (i.e., 70NR30PE/DCP) were found to be less prone to creep, as ex-

pected, but still deformed rapidly at stresses near to 1 MPa. A limited number of experiments were conducted with dead weight loading at stresses sufficiently small to reduce creep to an acceptably low level during a 2-week UV exposure for comparison with the stress-relaxation UV exposure trials.

The ozone levels were checked at various sites within the room in which the UV trials were conducted, including positions close to the samples under test, and found to be below the measurement threshold for the equipment used (<0.02 ppm). In the earlier studies conducted by Marcos Mailló and White,<sup>20</sup> it was discovered that when a simple shield made from aluminum foil prevented UV reaching part of the sample surface, there was a very sudden demarcation between the degradation displayed by the exposed and unexposed zones, respectively. The shield was loosely attached, and it was inconceivable that the ozone concentration above the sample surface on either side of the shield boundary was different, leading to the conclusion that photo-oxidation rather than ozone attack was principally responsible for the degradation. In the trials conducted for this investigation, this simple yet effective device (of shielding part of the sample from direct UV exposure) was adopted as routine.

### Surface degradation analysis

Samples were inspected with light optical microscopy and scanning electron microscopy (SEM) at intervals during the photodegradation experiments. Although it is possible to view rubber samples in the SEM without modification,<sup>25</sup> a sputtered gold coating was applied to improve image quality.

Oxidation of rubber samples often results in the formation of cracks or fissures on the surface. These often appear during exposure if this is conducted under tensile stress. If the component is then removed from the stressing jig (or the assembly that holds it in tension in service), the cracks close up and are rendered less visible or sometimes invisible. Therefore, for microscopic examination it is beneficial to mount the sample in a miniature straining device that can be placed on the microscope stage and apply a small strain during observation.<sup>20</sup> In addition to using this device to reopen cracks formed during tensile exposures, we also used it to apply a small strain to samples that were exposed unstrained. For many samples, this caused the appearance of a pattern of cracks. We cannot be certain whether or not these cracks were present before deformation on the microscope stage. If they were present, they might have been caused by mishandling or even by deformation under the weight of the sample itself. Alternatively, they may be produced simply by the deformation on the microscope stage. Whatever the precise origin of the cracking

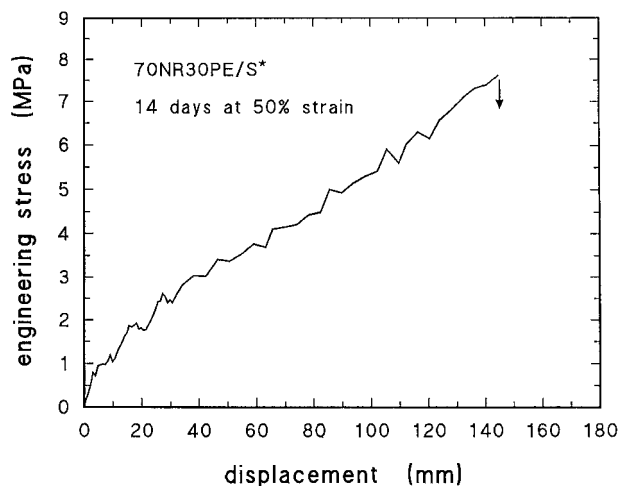


**Figure 1** Load-deformation relationship for a 70NR30PE/S\* sample after holding at 50% extension for 14 days (unexposed).

observed, the size and number of the cracks varied with the severity of the exposure and provided a useful assessment of the degradation caused. Oblique illumination was used, and the direction of the light impinging on the specimen surface was adjusted to give the greatest visibility of the cracks.

Samples that broke during UV exposure under stress-relaxation conditions were mounted on SEM stubs, fracture surface upward, permitting observation of all four faces and the fracture surface by appropriate positioning with the SEM stage controls. For SEM observation of samples that did not break during exposure, a small platform was made that could be mounted in the specimen stage and that had two simple clamps between which samples could be stretched and held in the strained state for gold coating and subsequent inspection in the SEM. As with the equivalent device for the light optical microscope, this held the cracks open for maximum visibility. The secondary electron image was used throughout, and we found that satisfactory images could be obtained with a 15-kV accelerating potential.

### Mechanical testing

After UV exposure, the strips (100 × 12mm) were tensile tested on an Instron 4500 tensile test machine with a grip separation of 60 mm and a crosshead speed of 500 mm/min. The load-deformation traces were sometimes quite noisy, possibly because the load cell was operating near to its sensitivity limit. In some cases, we observed that stretch marks formed on the surface of the sample during tensile testing and that localized fracture of these drawn regions occurred one by one, leading to a stick-slip behavior that was clearly recognizable on the load-deformation trace (Fig. 1). This effect and the noise were smoothed out

for the presentation of results in Figure 12 (shown later).

## RESULTS

### General observations

Although there were detailed differences in the behavior of the different materials, most of them were light brown in color and became clearer during UV exposure. The surfaces were shiny and tacky in the unexposed state but the UV-exposed surfaces became dull and less sticky. We often observed that samples that were exposed to UV in the stress-relaxation frames developed cracks perpendicular to the stress axis during exposure. The samples were usually curved after release from the frames, and the exposed surface sometimes showed a rippled appearance. The curvature was convex on the exposed surface and amounted to as much as 270° over the full length of the coupon. An exception was obtained with 60NR40PE, for which curvature was obtained after 7 and 14 days exposure at 25% strain and after 7 days at 50% strain, but no noticeable curvature was present after the sample was released after 14 days exposure at 50% strain. For this sample (14 days exposure at 50% strain), cracks also formed in the unexposed face. When samples that had been exposed in the stress-relaxation frames were viewed under the microscope, fine cracks oriented parallel to the stress axis were often visible.

Cracks developed in the unexposed surface with some samples.

### Surface degradation

#### 70NR30PE and 60NR40PE

The basic grade blend, 70NR30PE, showed surface cracking after 7 days unstrained exposure. The cracks became more visible on the application of 50% strain on the microscope stage.

Extending the (unstrained) exposure period to 14 days did not cause very much difference in the appearance of the surface. In Figure 2, the appearance of the surface of a sample exposed for 14 days unstrained is compared with that seen when a 50% strain was imposed by the stage jig. Exposure in stress relaxation (25% strain) for 7 days resulted in a pattern that was not very different (Fig. 3). 70NR30PE samples exposed to UV in uniaxial stress relaxation at 50% strain broke after 5–6 days but were left under UV exposure until a total of 7 days had elapsed. Figure 4 shows the surface of such a sample: the cracks had a much greater tendency to be inclined to the normal to the stress axis than in the samples pictured in Figures 2 and 3, giving a mosaic appearance. The cracks on the

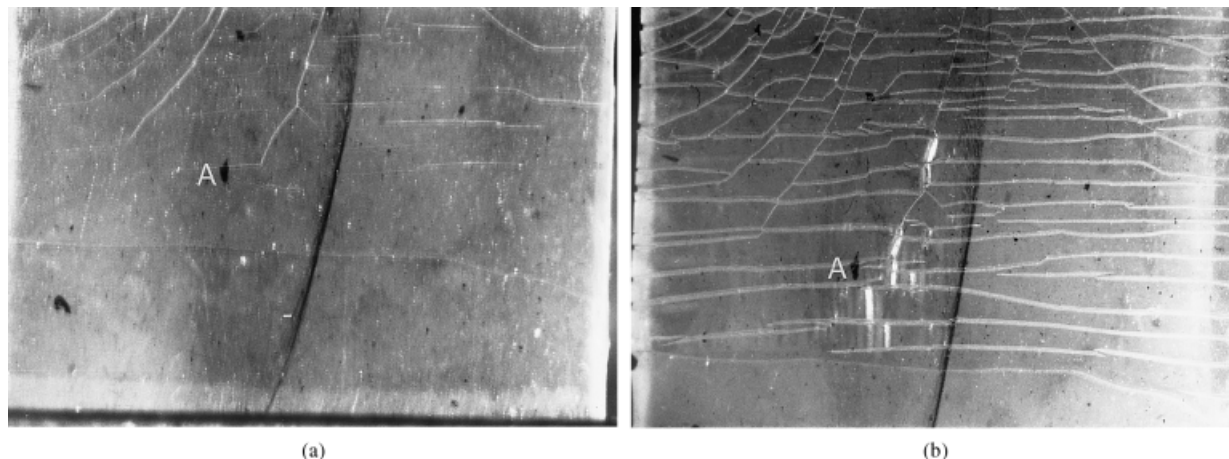


**Figure 2** (a) Surface of 70NR30PE after 14 days unstrained exposure to UV irradiation and (b) the same surface after straining approximately 50% on the microscope stage. The field of view is shifted somewhat: the piece of dirt at position A in both micrographs is the same.

exposed surface were wide and deep, especially when the sample was strained on the microscope jig, whereas on the unexposed surface, hairline cracks were found.

After unstrained UV exposure for 7 days, 60NR40PE showed somewhat more cracking when strained for microscopy than did the corresponding 70NR30PE sample [Fig. 5(a)], but after 14 days of unstrained exposure, the cracks formed in the microscope straining jig were fewer but more regular and on average a little larger than those in 14-day 70NR30PE [Fig. 5(b)]. After exposure in tensile stress relaxation at 25% strain, the cracking pattern in 60NR40PE under light optical observation was rather similar to that in obtained after 14 days of unstrained exposure. After 14 days of exposure, the appearance was totally different, however, and a dense pattern of fine cracks was observed, covering the surface (Fig. 6). As with 70NR30PE, when 60NR40PE was exposed in tensile stress relaxation at 50% strain, some cracks

formed parallel to the strain axis (Fig. 7). Unlike 70NR30PE, 60NR40PE survived a 14-day exposure at this strain, after which cracking was visible on the reverse side as well as the exposed side.

#### 70NR30PE/DCP and 70NR30PE/S\*

Use of a crosslinking agent produced significant changes in the appearance of the samples after exposure and stretching on the light microscope straining jig. After 7 days of unstrained exposure, 70NR30PE/DCP showed a much finer network of cracks than did 70NR30PE under the same conditions [Fig. 8(a)]. After 14 days of unstrained exposure, the cracks that formed under strained observation were fewer and deeper [Fig. 8(b)], reminiscent of the behavior observed with 60NR40PE. After 7 days of unstrained exposure, 70NR30PE/S\* showed rather more cracking than average under these conditions (Fig. 9), but after 14 days, the cracks that formed were larger, and the spacing

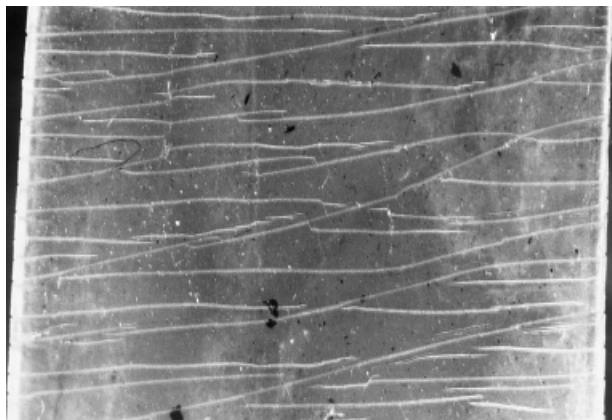


**Figure 3** Surface of 70NR30PE after exposure to UV irradiation under 25% tensile strain, strained approximately 50% on the microscope stage.

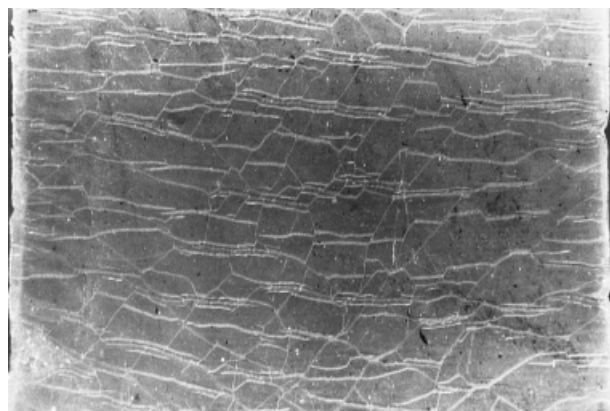


**Figure 4** Surface of 70NR30PE after 7 days exposure to UV irradiation under 50% tensile strain, strained approximately 50% on the microscope stage.

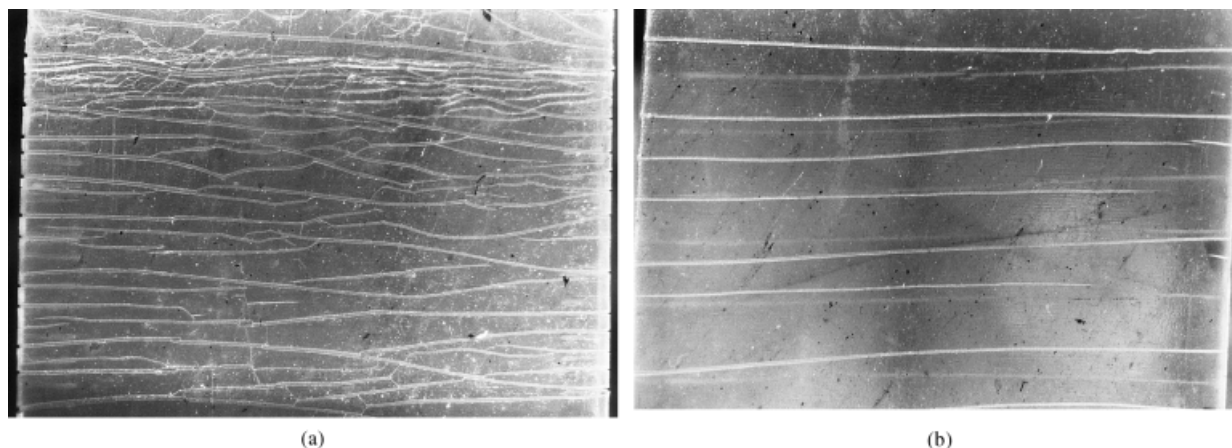


**Figure 5** Surface of 60NR40PE after unstrained exposure to UV irradiation: (a) 7 and (b) 14 days (both strained approximately 50% on the microscope stage).

between them was much greater (Fig. 10). (N.B. Fig. 10 shows also the effect of screening part of the surface from UV: the cracking referred to here was in the unshielded part in this sample.)

Exposure of 70NR30PE/DCP for 7 days under tensile stress relaxation at 25% strain produced a finer cracking pattern with a fairly conventional appearance, but after 14 days, a major crack had developed, extending across most of the sample width. At 50% strain, the samples broke within 2–3 days of UV exposure.

Cracks were not visible on the surface of 70NR30PE/S\* until the sample was observed on the straining microscope stage. Samples exposed to UV in the straining rigs showed cracking on the exposed surface and severe curvature and rippling (both 7-day and 14-day exposures and both 25 and 50% deformation).

#### Homopolymers

Both homopolymers were compounded with DCP. Unlike the blends, the surfaces of NR/DCP became

more sticky and shiny during both unstrained and strained UV exposure. After UV exposure in stress relaxation, the NR/DCP samples became very fragile. There was evidence of flow in the gauge length.

LDPE/DCP is not elastomeric and behaved quite differently to the blends. It did not show surface cracking of the kind discussed previously for the blends.

#### Effect of the shield

The part of the surface beneath the shield showed greatly reduced degradation. An example is illustrated in Figure 10, which shows the surface of a 70NR30PE/S\* sample after 14 days of unstressed exposure. There is a clear demarcation at the shadow boundary. Another interesting feature is that the sample width was less within the shadow than in the unprotected region (both edges of the sample are in view in Fig. 10). This was attributed to Poisson shrinkage transverse to the strain applied for microscopic observations and implies that the shadowed region

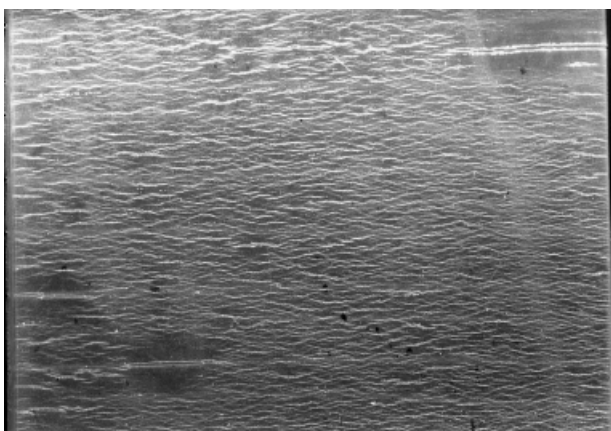


**Figure 6** Surface of 60NR40PE after 14 days exposure to UV irradiation under 25% tensile strain, strained approximately 50% on the microscope stage.

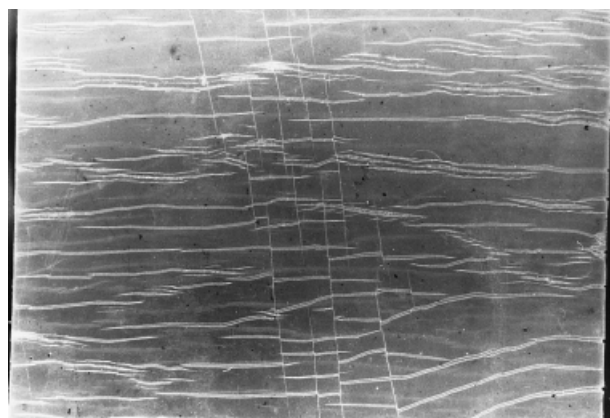


**Figure 7** Surface of 60NR40PE after 7 days exposure to UV irradiation under 50% tensile strain, strained approximately 50% on the microscope stage.

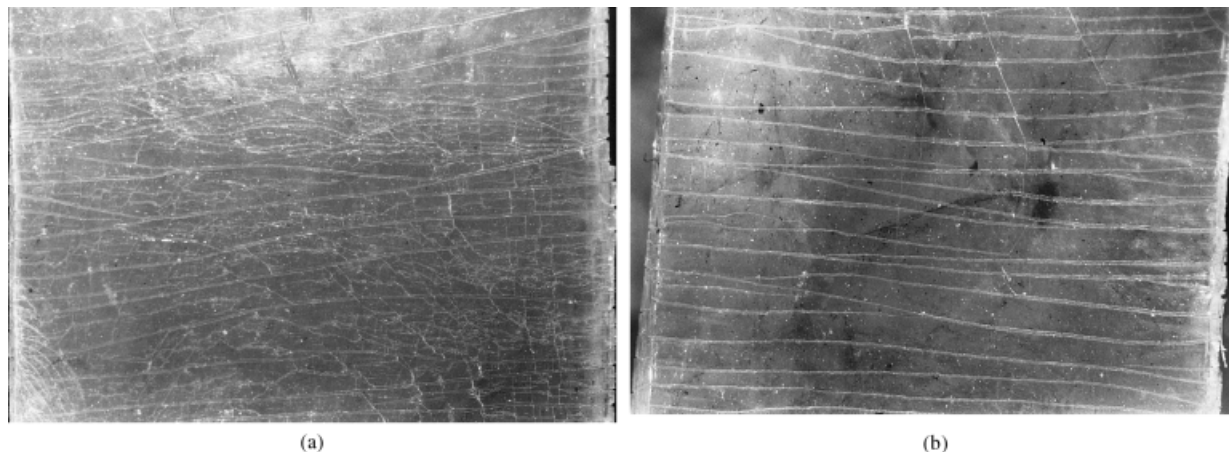


**Figure 8** Surface of 70NR30PE/DCP after unstrained exposure to UV irradiation: (a) 7 and (b) 14 days (both strained approximately 50% on the microscope stage).

had lower stiffness than the exposed portion, as would be expected if crosslinking had occurred preferentially in the exposed part.

#### SEM observations

More details of the crack geometry were revealed by SEM. Figure 11(a) shows a typical cracking pattern on the surface of 70NR30PE when it was strained on the SEM microscope stage after 7 days of unstrained exposure. Most of the cracks had the appearance shown in Figure 11(b) at high magnification, but in some cracks, fibrils were found to have drawn between the crack surfaces, giving the appearance of a coarse, low-density craze [Fig. 11(c)]. Both types of crack could coexist in close proximity [Fig. 11(d)].

#### Mechanical properties

The results of the tensile tests are shown in Figure 12. 70NR30PE samples conditioned for 14 days in the

dark in the constant temperature room extended to nearly 2.5 times the original length before breaking [Fig. 12(a)]. The sample that was held at 25% extension in the dark for the same period of time was slightly stiffer, with a higher load recorded at all displacements during the tensile test, and failed at approximately the same strain. The sample that was held at 50% extension in the dark for 14 days was stiffer still but failed at a lower extension (after extending approximately 100%). The samples exposed to UV at 50% strain broke before 14 days had elapsed. A fairly similar pattern of behavior was observed with 60NR40PE [Fig. 12(b)]. The sample conditioned unstrained in the dark gave the largest elongation to break. The samples held extended but kept in the dark became stiffer and failed at lower extension, with greater effect with 50% extension than with 25% extension. UV exposure in the unstrained state resulted in lower stiffness than observed in the unstrained and

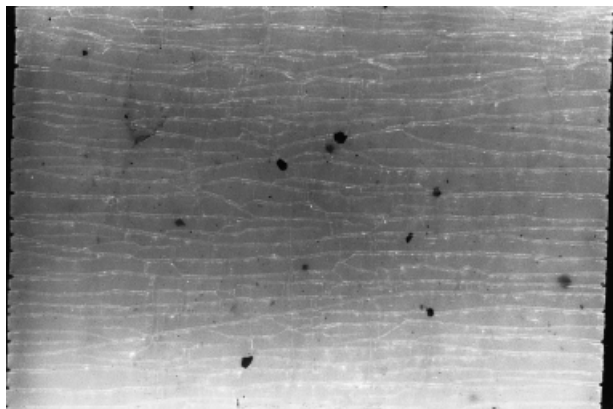


**Figure 9** Surface of 70NR30PE/S\* after 7 days unstrained exposure to UV irradiation (strained approximately 50% on the microscope stage).

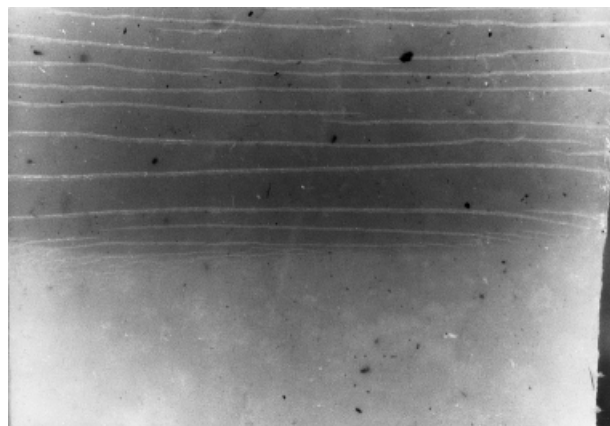


**Figure 10** Surface of 70NR30PE/S\* after 14 days unstrained exposure to UV irradiation (strained approximately 50% on the microscope stage). Part of the shielded region is shown: the demarcation between shielded and unshielded regions is very clear.

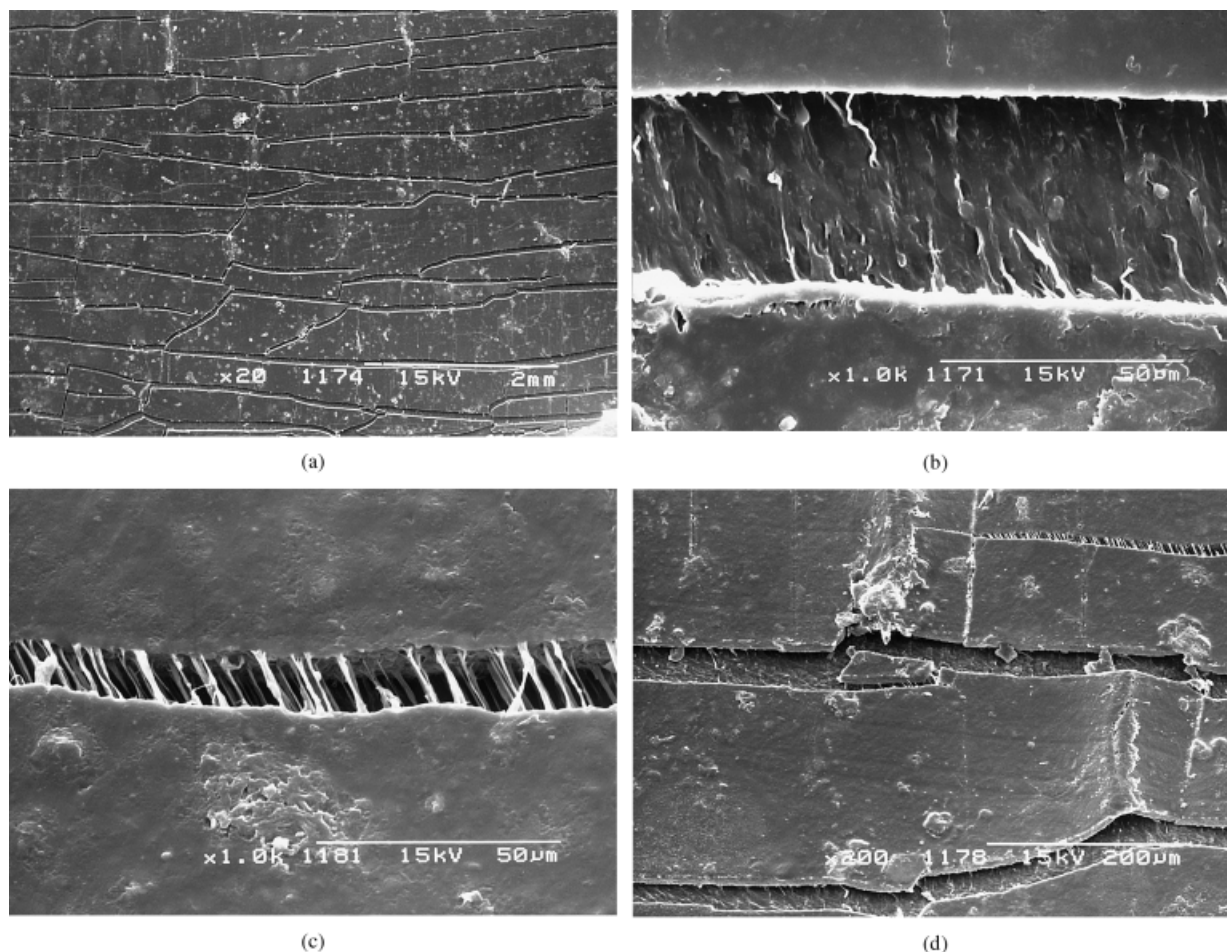


**Figure 11** Surface of 70NR30PE after 7 days unstrained exposure to UV irradiation, observed in the SEM while mounted on the straining rig: (a) low-magnification view, (b) a crack with a rather featureless appearance, (c) a crack with craze-like morphology, and (d) a region containing both kind of cracks.

unexposed sample, but exposure under tension produced increased stiffness. Exposed samples failed at lower extensions than any of the unexposed samples, and failure was observed to occur at progressively lower extensions as the preconditioning strain increased.

The samples containing crosslinking agent were stiffer than 70NR30PE, as expected [Fig. 12(c,d)]. 70NR30PE/DCP samples exposed to UV in the strained state failed before 14 days had elapsed. The sample conditioned for 14 days in the dark while extended 25% in the dark showed a greater extension during the subsequent tensile test than the unexposed and unstrained sample, but after 14 days at 50% strain in the dark, the sample became less stiff and failed at a lower extension, in contrast to 70NR30PE. As with samples made from 70NR30PE, the effect of UV exposure was to reduce stiffness and extension to break. The effect of preconditioning on the tensile behavior of 70NR30PS/S\* was not as marked as with the other compositions [Fig. 12(d)]. The tensile behavior of samples preconditioned under UV and in the dark at 50%

strain was not significantly different from that obtained with the sample exposed to UV for 14 days at 25% strain.

## DISCUSSION

### Degradation mechanisms and cracking patterns

The most likely explanation for the curvature that developed in many of the samples as the result of UV exposure while under tensile strain is as follows. Strained molecules are likely to suffer photo-oxidative scission. The individual broken fragments will not contract as much when the stress is removed; so when the sample was removed from the straining rig, the exposed surface contracted less than the unexposed surface, which suffered less change and retained more of its rubbery properties. Such differential contraction will cause curvature in the sense observed. If cracking occurs in the strained state, this will lead the way to even greater irreversible deformation because creep extension will take place at the crack roots; when the

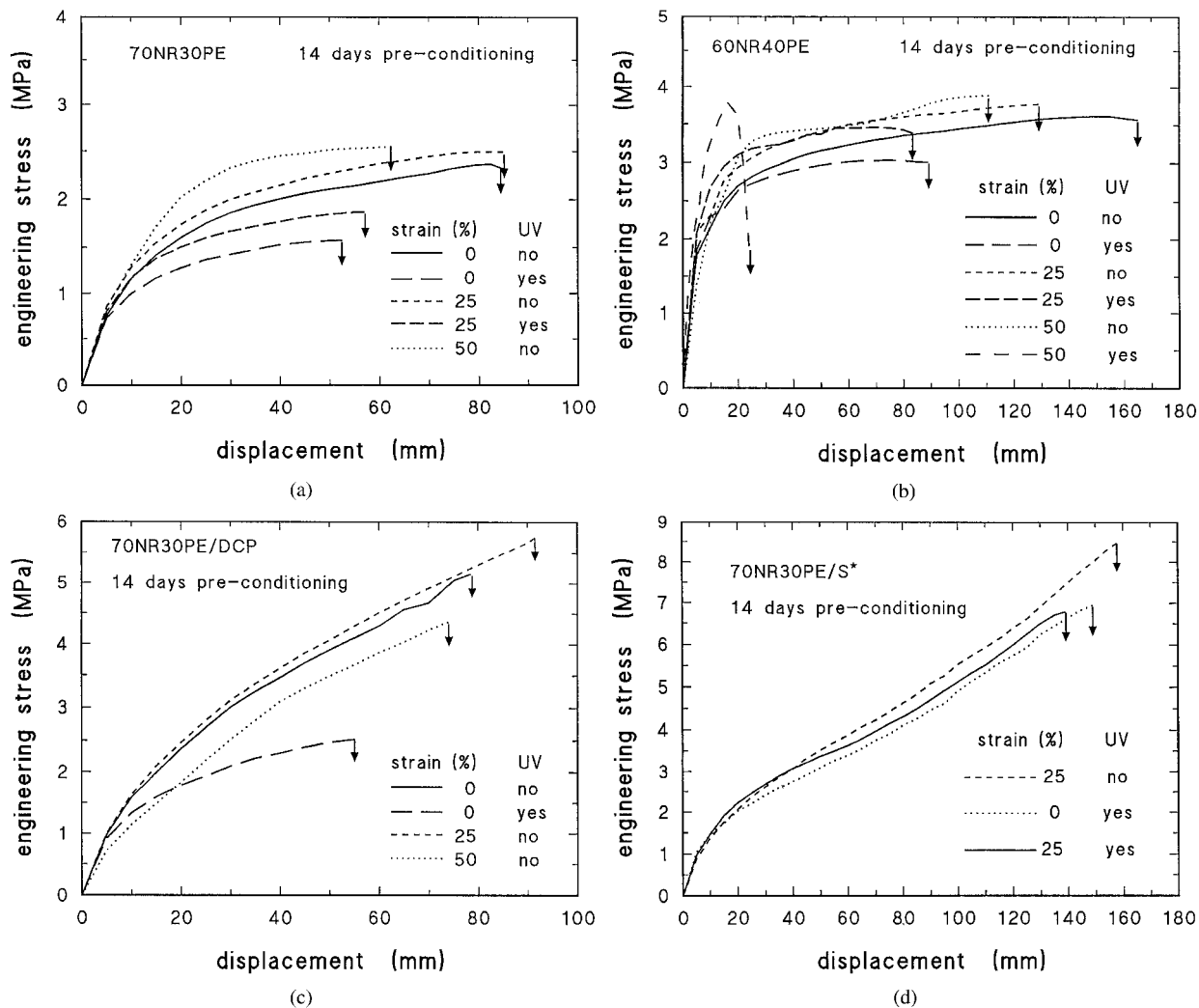


**Figure 12** Load-deformation curves for blends after conditioning for 14 days under various combinations of strain and UV irradiation exposure: (a) 70NR30PE, (b) 60NR40PE, (c) 70NR30PE/DCP, and (d) 70NR30PE/S\*.

sample is released from the straining rig and contraction of the rubbery material near the unexposed face occurs, the cracks are not able to close completely because of the deformation at the roots. The flat-bottomed appearance of cracks in many of the light optical and SEM micrographs provided evidence for this. This incomplete crack closing may contribute to the rippling effect observed in some samples. Indeed, cracks were sometimes visible, clearly associated with the ripples (Fig. 13). Pronounced curvature and rippling were not seen in samples that developed cracking in the unexposed face as well as the exposed surface, presumably because changes in the unexposed face balanced those in the exposed face. The axial contraction that occurs when samples are released from the stress-relaxation frames is accompanied by (Poisson) expansion in transverse directions, and this probably causes the cracking parallel to the stress axis.

The unusual stick-slip type of load-deformation behavior observed in tensile tests on UV-degraded sam-

ples, described in the Mechanical Testing section and illustrated in Figure 1, demands some explanation. It has been shown elsewhere that the blends have PE as the matrix and rubber as the dispersed phase.<sup>22</sup> It is not known whether the two components, which have widely different stiffnesses, deform in an affine manner, but if they do, the one that loses its ductility first can be expected to fail first. We speculate that crosslinking in the PE phase caused by UV irradiation reduced its deformability, and it was no longer able to draw as much as the rubber phase, which retained its high deformability. If this is the case, cracks formed in the PE matrix to allow the underlying rubber zones take up a larger deformation (Fig. 14). Each time cracks appeared in the PE matrix, some unloading occurred because a larger fraction of the deformation was taken up by the softer rubbery phase. The stress redistributed over the intact load-bearing material and climbed with continued deformation as the test proceeded until another part of the PE matrix reached the critical condition and cracked. This process was re-



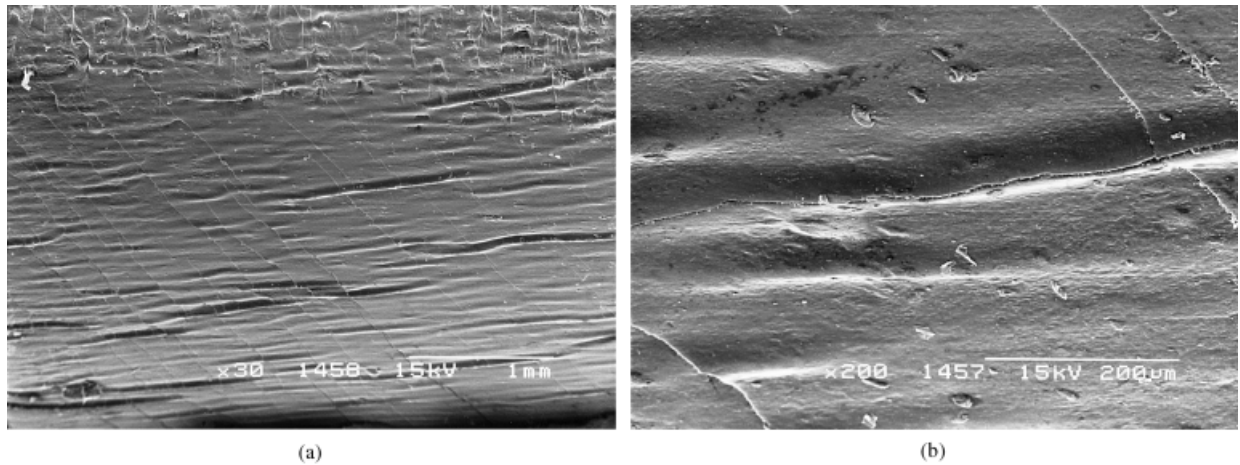
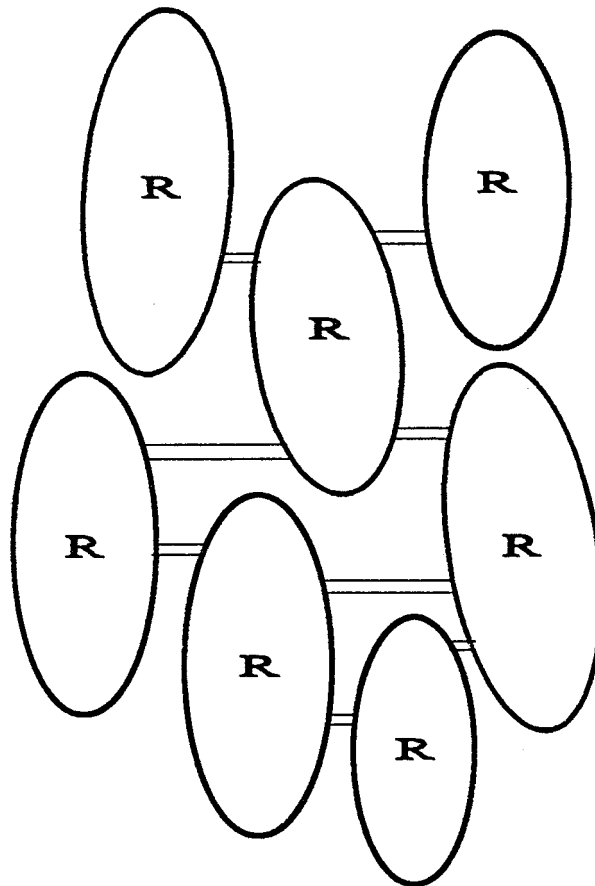


**Figure 13** Rippled surface on 70NR30PE after strained exposure: (a) low magnification and (b) high magnification.

peated until a continuous crack path was produced across the test-piece section, probably when deformation in the rubbery zones reached a critical state, allowing fracture to proceed through them to enable the cracks in the PE to join up.

When a shield prevented UV reaching part of the surface directly, there was a clear demarcation between surface degradation at the boundary between the exposed and unexposed regions. This provided powerful confirmation that UV rather than ozone was



R : Rubber Phase

= : cracks in PE phase, opened up to permit deformation in the rubber phase

**Figure 14** Schematic of a cross-section through a strained blend showing rubbery domains (R) stretched parallel to the tensile axis, embedded in a PE matrix that has begun to crack.

the main agent of oxidation under the conditions used in these trials. This result is similar to that found before when a NR/butadiene rubber blend was tested.<sup>20</sup>

Cracking developed in the surfaces of the blends when exposed to UV under 25 or 50% extension. The cracking patterns developed under continuous loading and UV exposure were sometimes different from those obtained in the surface of samples that were exposed to UV in an unstrained state and were subsequently deformed. The geometry of the cracking pattern of a coating on the surface of a thick substrate is complex and depends on the properties and the thickness of the coating, the adhesion between the coating and the substrate, the size and distribution of defects in the coating, and the loading conditions.<sup>26-31</sup> The degraded layer can be considered to behave like a coating, but its properties change with exposure, and there are too many unknowns to make a quantitative assessment of the pattern geometries at this time.

### Effect of composition

The observations made with the homopolymers indicate that the NR was degraded by UV much more readily than PE. The degradability of the blends was intermediate between the homopolymers. It was not possible to rank 60NR40PE above 70NR30PE with certainty. The effect of including a crosslinking agent was to cause the formation of finer cracking patterns and to require longer exposure to provoke a given level of surface degradation.

### Mechanism of degradation

The use of a shield showed very clearly that direct UV exposure was required to produce the rapid degradation observed in these tests. Although UV is known to produce ozone from atmospheric oxygen, it is almost inconceivable that the ozone level just inside the shadow was very different from that in the exposed region. Ozone diffusion in air is much easier than through solid samples. Therefore, although a contribution to degradation from ozone attack could not be ruled out, it is evident that the major contribution was due to photo-oxidation.

## CONCLUSIONS

A new family of thermoplastic elastomers, based on blends between NR and LDPE, were shown to degrade significantly under UV exposure. Photo-oxidation rather than ozone degradation was found to be the major mechanism, even with samples held in tension. Under the test conditions applied here, the blends were more resistant than the NR homopoly-

mer. Given that the weatherability of NR and of PE can be improved spectacularly by appropriate additives and/or by compounding with Carbon Black or other fillers, this is most encouraging. A preliminary study of the effect of adding stabilizers was given elsewhere.<sup>21</sup> Introducing crosslinks (at low concentration so that the thermoplastic nature of the blends was retained) improved the resistance to photo-oxidation when the crosslinking system consisted of zinc oxide, stearic acid, sulfur, mercaptobenzothiazole (MBT), and tetramethyl thiuram disulfide (TMTD).

## References

1. Bhowmick, A. K.; Stephens, H. L., Eds. *Handbook of Elastomers: New Developments and Technology*; Marcel Dekker: New York, 1998.
2. De, S. K.; Bhowmick, A. K., Eds. *Thermoplastic Elastomers from Rubber-Plastic Blends*; Horwood: Chichester, England, 1990.
3. Coran, A. Y.; Patel, R. U.S. Pat. 4,104,210 (1978).
4. Roy Choudhury, N.; Bhowmick, A. K. *J Appl Polym Sci* 1989, 38, 1091.
5. Jha, A.; Bhowmick, A. K. *Rubber Chem Technol* 1997, 70, 798.
6. Ginic-Markovic, M.; Roy Choudhury, N.; Dimopoulos, M.; Matisons, J. G. *Polym Degrad Stab* 2000, 69, 157.
7. Davis, A.; Sims, D. *Weathering of Polymers*; Applied Science: Barking, 1983.
8. Braden, M.; Gent, A. N. *J Appl Polym Sci* 1960, 3, 90.
9. Braden, M.; Gent, A. N. *J Appl Polym Sci* 1960, 3, 100.
10. Andrews, E. H. *J Appl Polym Sci* 1966, 10, 47.
11. Doyle, M. J. *Rubber Plast News* 1997, (Sept), 69.
12. Adam, C.; Lacoste, J.; Lemaire, J. *Polym Degrad Stab* 1989, 24, 185.
13. Adam, C.; Lacoste, J.; Lemaire, J. *Polym Degrad Stab* 1990, 29, 305.
14. Adam, C.; Lacoste, J.; Lemaire, J. *Polym Degrad Stab* 1991, 32, 51.
15. Adam, C.; Lacoste, J.; Siampiringue, N.; Lemaire, J. *Eur Polym J* 1994, 30, 433.
16. Dunn, J. R. *J Appl Polym Sci* 1960, 4, 151.
17. O'Donnell, B.; White, J. R. *Polym Degrad Stab* 1994, 44, 211.
18. O'Donnell, B.; White, J. R. *J Mater Sci* 1994, 29, 3955.
19. Tong, L.; White, J. R. *Polym Degrad Stab* 1996, 53, 381.
20. Marcos Maillou, C.; White, J. R. *Plast Rubber Compos* 1999, 28, 277.
21. Bhowmick, A. K.; Heslop, J.; White, J. R. *Polym Degrad Stab* 2001, 74, 513.
22. Bhowmick, A. K.; White, J. R. *J Mater Sci*, to appear.
23. Qayyum, M. M.; White, J. R. *J Mater Sci* 1985, 20, 2557.
24. Qayyum, M. M.; Davis, A. *Polym Degrad Stab* 1984, 6, 201.
25. White, J. R. In *Fractography of Rubbers*; Bhowmick, A. K.; De, S. K., Eds.; Elsevier Applied Science: Barking, 1991; Chapter 2.
26. Hornig, T.; Sokolov, I. M.; Blumen, A. *Phys Rev E* 1996, 54, 4293.
27. Leterrier, Y.; Boogh, L.; Andersons, J.; Månson, J.-A. E. *J Polym Sci Part B: Polym Phys* 1997, 35, 1449.
28. Leterrier, Y.; Andersons, J.; Pitton, Y.; Månson, J.-A. E. *J Polym Sci Part B: Polym Phys* 1997, 35, 1463.
29. Handge, U. A.; Solokov, I. M.; Blumen, A.; Kolb, E.; Clément, E. *J Macromol Sci Phys B* 1999, 38, 971.
30. Handge, U. A.; Solokov, I. M.; Blumen, A. *Phys Rev E* 2000, 61, 3216.
31. Handge, U. A.; Solokov, I. M.; Blumen, A. *J Phys Chem B* 2000, 104, 3886.